ELSEVIER

Journal of Chromatography A, 880 (2000) 203–232

JOURNAL OF
CHROMATOGRAPHY A

www.elsevier.com/locate/chroma

Review

On-line identification of phytochemical constituents in botanical extracts by combined high-performance liquid chromatographic–diode array detection–mass spectrometric techniques

Xian-Guo He

Research Laboratory of Natural Products Chemistry, A. M. Todd Botanicals, 4091 West 11th Avenue, Eugene, OR 97402, USA

Abstract

It is necessary to determine all of the phytochemical constituents of botanical extracts in order to ensure the reliability and repeatability of pharmacological and clinical research, to understand their bioactivities and possible side effects of active compounds and to enhance product quality control. HPLC chromatographic fingerprints can be applied for this kind of documentation. Combined HPLC-diode array detection–MS techniques can provide on-line UV and MS information for each peak in a chromatogram. In most cases, direct identification of the peaks is possible, based on comparison with published data or with standard compounds. This review will primarily focus on electrospray and thermospray ionization MS and their applications for the qualitative analyses of phenolic compounds, saponins, alkaloids and other classes of natural products in botanical extracts. Twenty-one of the most commonly used herbal examples, their phytochemical analyses and characteristics of their mass spectra are described.

Keywords: Reviews; Plant materials; Phenolic compounds; Flavonoids; Saponins; Alkaloids

Contents

0021-9673/00/$ – see front matter
PII: S0021-9673(00)00059-5

1. Introduction

1.1. The complete herbal extract is the active ‘compound’

There has recently been an explosion of interest in herbal medicine throughout the world, and in the USA, the herbal supplements industry has grown into the mainstream market. Although they are still categorized as ‘dietary supplements,’ not regulated as drugs by the US Food and Drug Administration, these alternative remedies demand a pharmaceutical level of assurance of efficacy and safety for their use. In response to this blending of the characteristics of foods and pharmaceuticals, a new term was coined: ‘neutraceuticals.’ Most dietary supplements are crude plant extracts, which comprise a complex mixture of different phytochemicals (plant secondary metabolites). The chemical nature of these constituents differs considerably between species. Even the same herbal extracts may vary depending on harvest season, plant origin, drying process and other factors. There are many ‘standardized herbal extracts’ on the market that provide a specified level of one or two chemical constituents. This determination, however, does not give a complete picture of an herbal product, because multiple constituents are usually responsible for its therapeutic effects. These work ‘synergistically’ and cannot be separated into active parts. Consequently, it is necessary to define all of the phytochemical constituents of botanical extracts in order to ensure the reliability and repeatability of clinical and pharmacological research, to understand bioactivities and possible adverse effects of active compounds, and to enhance product quality control. The full extract must be regarded as the active ‘compound.’

The concept of phytoequivalence was developed in Germany in order to ensure consistency of herbal products [1]. According to this concept, a chemical profile for an herbal product should be constructed and compared with the profile of a clinically proven reference product.

1.2. HPLC–diode array detection–MS for comprehensive peak identification

HPLC chromatographic fingerprints can be applied for documentation of complete herbal extracts. Combined HPLC–UV diode array detection (DAD)–MS techniques take advantage of chromatography as a separation method and both DAD and MS as an identification method. DAD and MS can provide on-line UV and MS information for each individual peak in a chromatogram. In most cases, we can identify these peaks directly on-line by comparison with literature data or with standard compounds.

1.3. LC–MS coupling

HPLC carries out a chromatographic separation of analytes prior to MS analysis; however, HPLC and MS have different operating conditions. HPLC operates using high flow-rates, high pressures and liquid-phase operation near room temperature; in contrast, MS uses low flow-rates, high vacuum and gas-phase operation at a higher temperature. Various interfaces overcome this difficulty and allow for on-line coupling of these two instruments [2].

The basis of mass spectrometry is the production of ions that are subsequently separated, or filtered according to their mass-to-charge (m/z) ratio and then detected [3]. A LC–MS interface must accomplish nebulization and vaporization of the eluate, ionization of the analyte, removal of the excess solvent vapor and extraction of the ions into the mass detector. There are many different interfaces available to approach this target.

Two interfaces used successfully and widely in the analysis of herbal extracts are electrospray (ESP) and thermospray (TSP). When a high potential is applied between a narrow bore capillary filled with a flowing liquid and a nearby plate, a mist of charged droplets is obtained. This phenomenon is known as electrospray or electric atomization [4]. The ions observed are typically protonated molecules. The major drawback to ESP is the maximum allowable flow-rate limit; for MS, the lower the flow-rate, the better the performance.

The thermospray interface is based on the formation of a mist of vapor and small droplets from a heated vaporizer tube [3]. By applying efficient pumping, up to 2 ml/min of aqueous solvents can be introduced into the TSP–MS system. With thermally labile ionic compounds, electrospray ionization (ESI) shows better performance than TSP. There are also reports of particle-beam (PB) interfaces used in the analyses of herbal extracts. PB interfaces are capable of an efficient analyte-enrichment and can also be used to obtain EI spectra [5].

1.4. Collision-induced dissociation and MS–MS methods

Both ESP and TSP are soft ionization methods and do not typically produce many fragments. This is useful in quantitative analysis or molecular mass determination, but is not very helpful for structure elucidation. This disadvantage can be overcome by collision-induced dissociation (CID) or collision activated dissociation (CAD) methods [6]. Fragmentation is induced in one of the high pressure regions of the ion passageway from source to mass analyzer. Fragment ions produced by CID are very efficiently transported into the mass analyzer and can be regarded as the simple man‘s MS–MS method. Of course, no parent ion selection is possible. With HPLC–MS, one can run one analysis without CID and another with CID to obtain fragments of all components [6].

CID is performed to enhance fragmentation of the analytes either at the ESP source (in-source CID) or in conjunction with tandem MS (MS–MS). Tandem MS is the practice of carrying out one mass-selective operation after another [6]. The first operation is to isolate a parent ion, and the second is to determine the mass/charge ratio of the product ions formed after CID of the parent ion. The above sequence of ion isolation and CID can be repeated many times in a process known as MS^n. Tandem MS and in-source CID both give very similar product-ion mass spectra. Several valuable review articles dealing with LC–TSP–MS and its application in the analysis of botanical extracts have been published [7–14], therefore, this review will focus on HPLC–ESI–MS. Here, a number of herbal examples are used to describe how HPLC–DAD–MS can be effectively applied to perform component identification in complex mixtures.

2. Phenolic compounds and flavonoids

Phenolics possess an aromatic ring bearing one or more hydroxyl substituents. There are many different basic skeletons; for example, hydroxycinnamic acids such as caffeic acid (in apple and Echinacea) contain a C_6–C_3 skeleton. Anthraquinones such as aloe-emodin (in aloe) have a C_6–C_2–C_6 skeleton. Flavonoids such as quercetin (in cherry and ginkgo) have C_6–C_3–C_6 skeletons. Catechins (in tea) are proanthocyanidin monomers, each also having a C_6–C_3–C_6 skeleton. Phenolics occur widely in the plant kingdom and demonstrate a variety of bioactivities. Physiologically, they may act as antioxidants or agents contributing to anticarcinogenic or cardio-protective actions [15]. Flavonoids are most successfully analyzed by HPLC–DAD–MS techniques. Many papers dealing with LC–MS analyses of flavonoids in lemon, berries and other fruits or vegetables have been published [16–30].

2.1. Red Clover: Trifolium pratense (Leguminosae)

Red Clover is a major forage plant and its extract is used as a flavor ingredient. Its isoflavone constituents have estrogenic properties. Thus, standardized extracts of Red Clover have been used particularly by women as dietary supplements for maintaining physical and emotional well-being during mid-life.

Fig. 1 shows a simultaneous HPLC–UV and HPLC–ESI-reconstructed TIC (total ion current) chromatogram of a 70% ethanol extract of Red Clover. Fig. 2 shows the chemical structures of flavonoids occurring in Red Clover. Four major Red Clover isoflavonoids were identified in our laboratory [31], based on their abundant $[M+H]^+$ and $[M+Na]^+$ ions, UV spectra, retention times and analysis of hydrolyzed products in comparison with that of standard compounds. They are ononin (**6**, P4), sissotrin (**8**, P6) and their aglycones formononetin (**5**, P10) and biochanin A (**7**, P11). In this review, P is used to represent peaks in the text, and the compound numbering is independent for each herbal example. Ononin (**6**) and sissotrin (**8**) both displayed abundant protonated aglycone ions $[M-162+H]^+$, indicating a hexosy moiety elimination.

Using the same techniques, the other peaks are identified as genistin (**4**, P1), hyperoside (**16**, P2), isoquercitrin (**15**, P3) and daidzein (**1**, P5). They all showed intense molecular ions $[M+H]^+$ and adduct ions $[M+Na]^+$. P7–9 are only tentatively identified.

Lin et al. have recently identified several flavonoid glycoside malonates in fresh Red Clover blossoms by HPLC–ESI–MS [32]. These malonyl glycosides are easily decomposed by heating and cannot be detected by TSP–MS analysis [20].

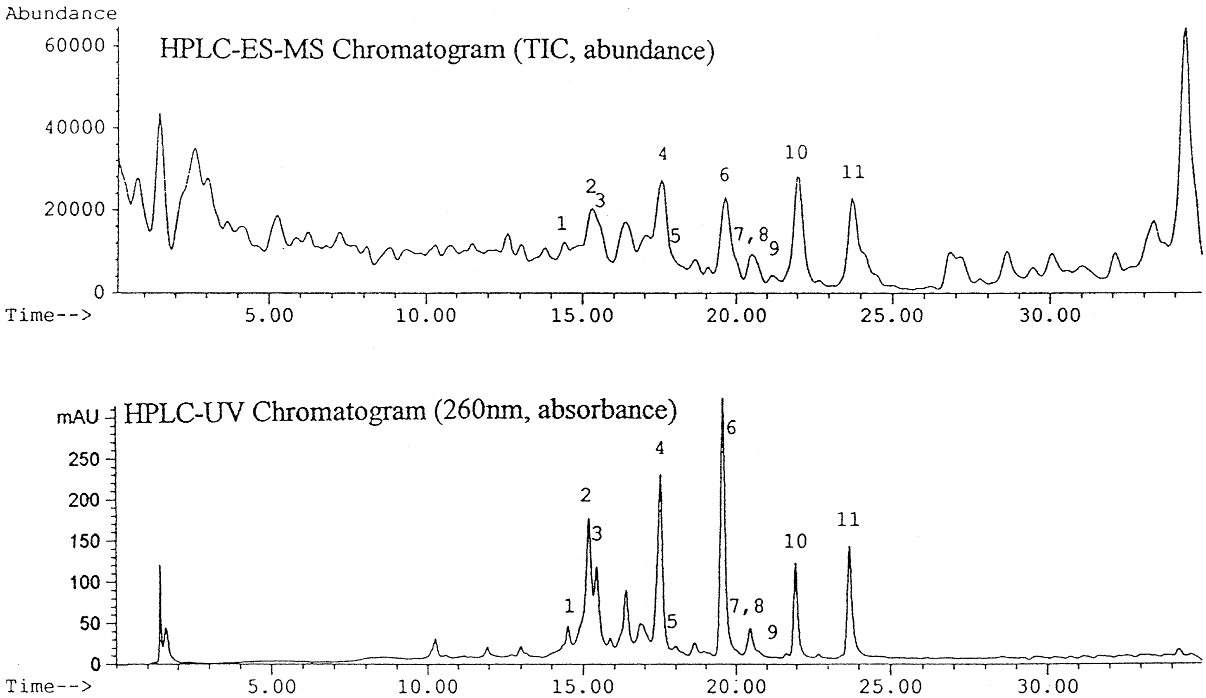

Fig. 1. Simultaneous HPLC–UV and HPLC-reconstructed total ion current (TIC) chromatogram of 70% ethanol extract of Red Clover, without post-column stream splitting. The following compounds are identified: P1 genistin (**4**); P2 hyperoside (**16**); P3 isoquercitrin (**15**); P4 ononin (**6**); P5 daidzein (**1**); P6 sissotrin (**8**); P7 pratensein (**12**); P8 pectolinarigenin (**11**); P9 pseudobaptigenin (**13**); P10 formononetin (**5**); P11 biochanin A (**7**). Time in min adapted from Ref. [30].

Isoflavone:

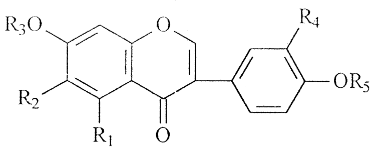

No.	Compound	R1	R2	R3	R4	R5	Mr
1	Daidzein	H	H	H	H	H	254
2	Daidzin	H	H	Glc	H	H	416
3	Genistein	OH	H	H	H	H	270
4	Genistin	OH	H	Glc	H	H	432
5	Formononetin	H	H	H	H	Me	268
6	Ononin	H	H	Glc	H	Me	430
7	BiochaninA	OH	H	H	H	Me	284
8	Sissotrin	OH	H	Glc	H	Me	446
9	Trifoside	OH	H	Me	H	Glc	446
10	Calycosin	H	H	H	OH	Me	284
11	Pectolinarigenin	OH	OMe	H	H	Me	314
12	Pratensein	OH	H	H	OH	Me	300
13	Psudobaptigenin	H	H	H	-O-	-CH2-	282

Flavonol:

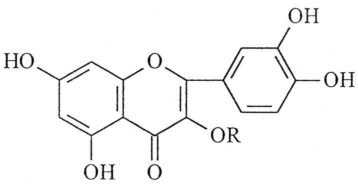

		R	Mr
14	Quercetin	H	302
15	Isoquercitrin	Glc	464
16	Hyperoside	Gla	464

Fig. 2. Structures of flavonoids in Red Clover.

Flavanone

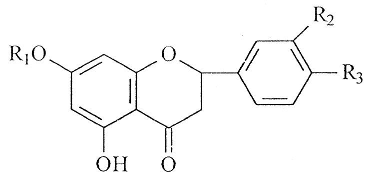

No.	Compound	R1	R2	R3	Mr
1	Isonaringin	rutinose	H	OH	580
2	Naringenin	H	H	OH	272
3	Naringin	neohesperidose	H	OH	272
4	Hesperitin	H	OH	OMe	302
5	Hesperidin	rutinose	OH	OMe	610
6	Neohsperidin	neohesperidose	OH	OMe	610

Flavone

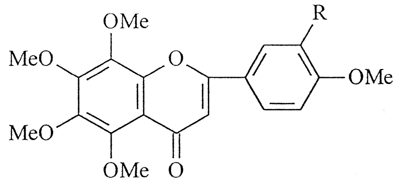

		R	Mr
7	Tangeritin	H	372
8	Nobiletin	OMe	402

Flavonol

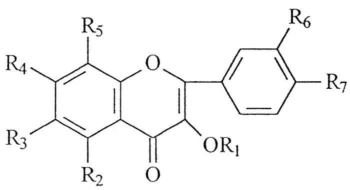

		R1	R2	R3	R4	R5	R6	R7	Mr
9	Auranetin	Me	H	OMe	OMe	OMe	H	OMe	372
10	Quercetin	H	OH	H	OH	H	OH	OH	302

Fig. 3. Structures of flavonoids in sour orange.

2.2. Sour orange: Citrus aurantium (Rutaceae)

Dried, immature sour orange fruit is a traditional Chinese medicine used to activate vital energy and circulation. Citrus flavonoids occur principally in the peel and more than 60 have been isolated. Three types of flavonoids occur in *Citrus* spp.: flavanones, flavones and flavonols. The flavanones predominate among the citrus flavonoids, with flavones and flavonols present in considerably smaller amounts. While the flavonoids in citrus usually occur as glycosides, the permethoxylated flavones are an exception: they occur as free aglycones.

The structures of flavonoids in *Citrus aurantium* are shown in Fig. 3. Five flavonoid standards naringin (**3**), hesperidin (**5**), neohesperidin (**6**), naringenin (**2**) and tangeritin (**7**) were analyzed by HPLC–DAD–ESI–MS in our laboratory [33]. Although the saturated flavanone diglycosides naringin (**3**), hesperidin (**5**) and neohesperidin (**6**) showed less ionization than the aglycone naringenin (**2**), their protonated molecular ions nevertheless are strong. Hesperidin (**5**) showed only a very weak protonated molecular ion $[M+H]^+$ at m/z 611 by TSP–MS (10% relative abundance), a major aglycone ion $[M\text{-rhamnoglucosyl}]^+$ at m/z 303 (100% relative abundance) and [M-rhammosyl]$^+$ at m/z 465 (8% relative abundance) [34]. This was probably due to the heating of TSP, resulting in loss of the terminal monosaccharide from hesperidin (**5**). ESI, however, operates without heat input during the spray ionization step, so there was no ion produced at m/z 465. Fig. 4 shows simultaneous HPLC–UV and TIC chromatograms of an 80% ethanol extract of sour orange. P2–7 and 11 are easily identified as isonaringin (**1**), naringin (**3**), hesperidin (**5**), neohesperidin (**6**), naringenin (**2**) and tangeritin (**7**), based on a comparison of their retention times, UV spectra and molecular ions with those of standard compounds and published data. The identity of P8 was confirmed

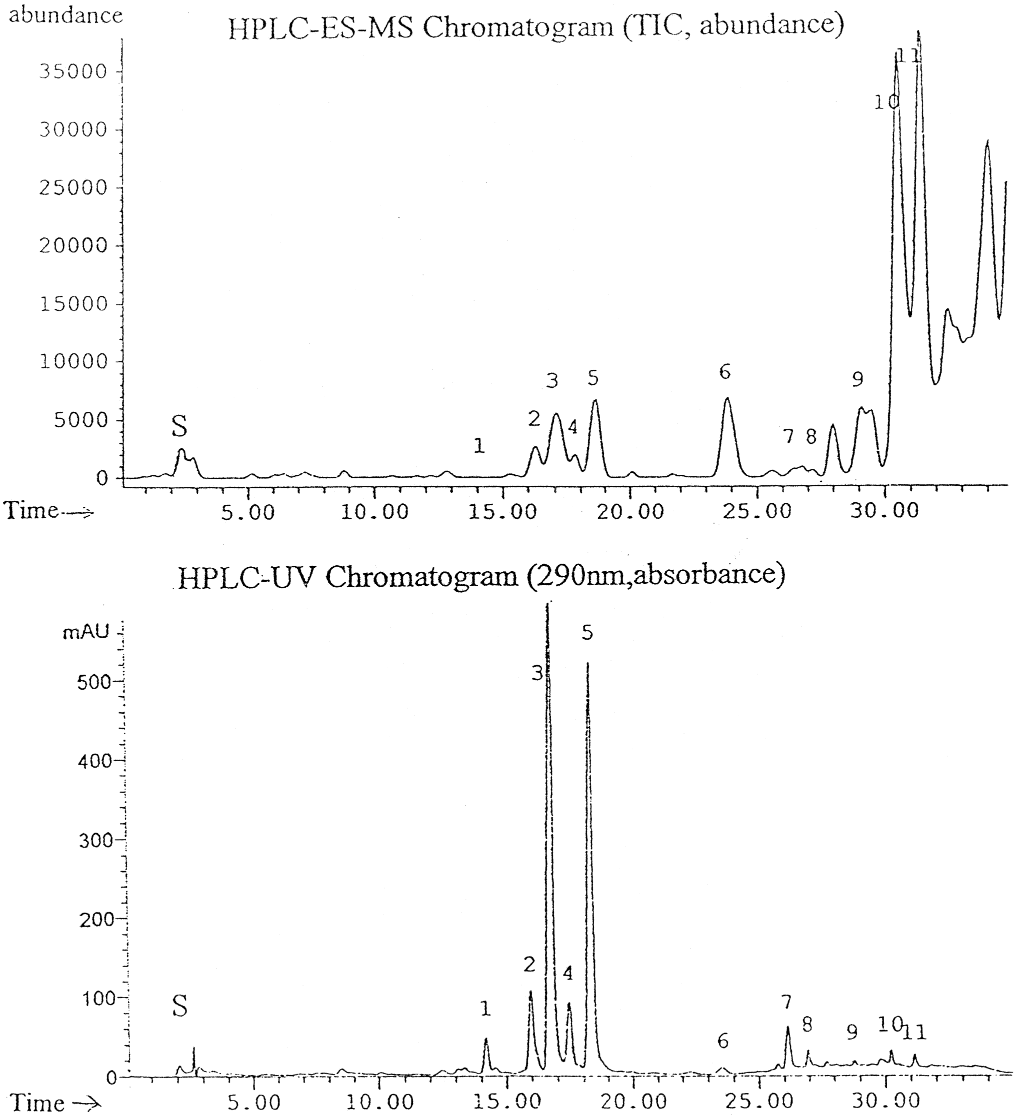

Fig. 4. Simultaneous HPLC–UV and HPLC-reconstructed TIC chromatogram of 80% ethanol extract of sour orange, without post-column stream splitting. The following compounds are identified: P1 naringin triglycoside*; P2 isonaringin (**1**); P3 naringin (**3**); P4 hesperidin (**5**); P5 neohesperidin (**6**); P7 naringenin (**2**); P8 hesperitin (**4**); P10 nobiletin (**8**)*; P11 tangeritin (**7**). Time in min. * Tentatively identified. Adapted from Ref. [33].

as hesperitin (**4**) following hydrolysis of hesperidin (**5**). P10 was tentatively identified as nobiletin (**8**).

The isomer pairs naringin (**3**) and isonaringin (**1**) and hesperidin (**5**) and neohesperidin (**6**) differ in the structure of the disaccharides attached at the 7-position. The rutinosides eluted prior to the respective neohesperidosides. P1 is still not identified; no ions were evident in this peak. Its retention time and UV spectrum are very close to that of a naringenin (**2**) triglycoside. In our experiments, we found that triglycoside is more difficult to ionize than diglycoside. Kiehne et al. reported quercetin triglycosides gave trisugars moiety signals of $[M+NH_4]^+$ at m/z 506 and $[M+NH_4 \cdot H_2O]^+$ at m/z 488 by LC–TSP–MS analysis [35].

2.3. St. John's Wort: Hypericum perforatum (Hypericaceae)

Since the Middle Ages, the extract made from the aerial portions of the St. John's Wort plant has had a well-known reputation as an anti-inflammatory agent. Today, it is considered primarily useful for antidepressive applications.

St. John's Wort contains a number of constituents with documented biological activities, including chlorogenic acid (**1**), flavonoids, naphthodianthrones, phloroglucinols and tannins. Thus, analysis of the entire extract is desirable. Brolis et al. successfully separated all the constituents within 50 min using a water–MeCN–MeOH–H_3PO_4 solvent system and an RP-18 column [36]. Since H_3PO_4 was not suitable for HPLC–MS operations, separation was performed in this study using aqueous 0.3% (v/v) formic acid without appreciable variation in the chromatographic profile. Fig. 5 shows its HPLC–UV profile with the HPLC–MS attributions of the component identified. Fig. 6 shows the chemical structures of some constituents in St. John's Wort.

P1 and P3 displayed identical UV spectra with maxima at 236 and 237 nm and gave $[M+H]^+$ ions at m/z 355 and $[M+H-H_2O]^+$ ions at m/z 337. P3 was identified as chlorogenic acid (**1**) by comparison with an authentic sample. P1 was therefore considered to be its isomer. P2 exhibited a $[M+H]^+$ ion at m/z 339 and a $[M+H\text{-}H_2O]^+$ ion at m/z 321. It allowed the identification of P2 as 3-O-*p*-coumaroylquinic acid as compared to UV data of chlorogenic acid (**1**).

P4–6 and P8 displayed identical UV spectra (typical of flavonols) with maxima at 259 and 355 nm. Moreover, an ion at m/z 303 indicated that they

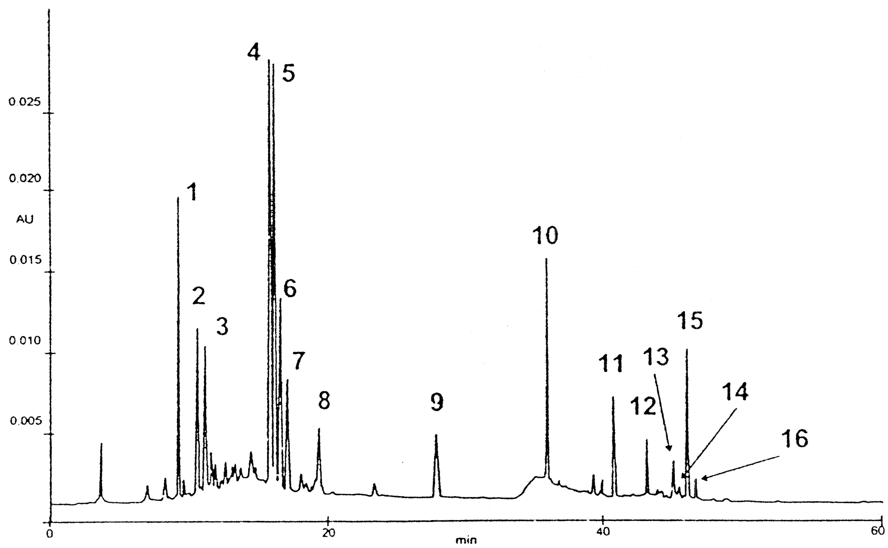

Fig. 5. Profile of St. John's Wort extract with the HPLC–MS attributions of the components detected. The following compounds are indicated: 1. chlorogenic acid isomer; 2. 3-*O*-*p*-coumaroylquinic acid; 3. chlorogenic acid (**1**); 4. rutin; 5. hyperoside; 6. isoquercitrin; 7. 3,3′,4′,5,7-pentahydroxyflavanone 7-*O*-rhamnopyranoside; 8. quercitrin: 9. quercetin 10. I 3.11 8 biapigenin (**2**); 11. pseudohypericin (**3**); 12. hypericin (**4**); 13. hyperforin analogue; 14. hyperforin analogue; 15. hyperforin (**5**); 16. adhyperforin (**6**). Adapted from Ref. [36].

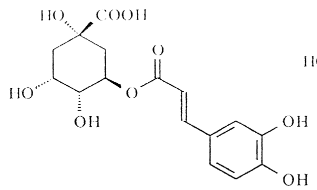

Chlorogenic acid (**1**) **Mr** 354

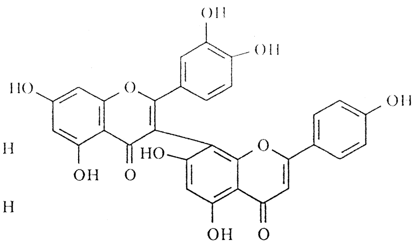

I 3 II 8-Biapigenin (**2**) **Mr** 538

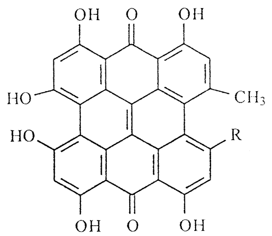

	R	**Mr**
Pseudohypericin (**3**)	CH2OH	520
Hypericin (**4**)	CH3	504

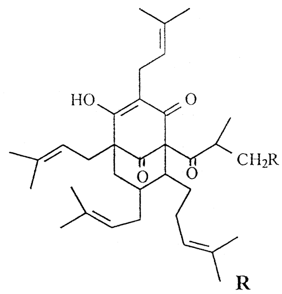

	R	**Mr**
Hyperforin (**5**)	H	536
Adhyperforin (**6**)	CH3	550

Fig. 6. Structures of some constituents in St. John's Wort.

are quercetin derivatives. P4, which exhibited $[M+H]^+$, $[M+Na]^+$ and $[M+K]^+$ ions at m/z 611, 633 and 649, respectively, and fragment ions at m/z 465 and 303 due to the successive loss of a deoxy-hexose unit and a hexose unit, was identified as rutin by comparison with the authentic sample. P5, which exhibited $[M+H]^+$, $[M+Na]^+$ and $[M+K]^+$ ions, at m/z 465, 487 and 503 respectively, and a fragment ion at m/z 303 due to the loss of a hexose unit, was identified as hyperoside by comparison with an authentic standard.

P6 and P8–10 were identified as isoquercitrin, quercitrin, quercetin and I3, II8-biapigenin (**2**) in the same manner. P7 displayed an UV spectrum with a maximum at 292 nm and a shoulder at 342 nm, indicating that it was a flavanone. It was tentatively identified as 3,3′,4′,5,7-pentahydroxyflavanone 7-*O*-rhamnopyranoside based on MS data.

P13–16 all displayed identical UV absorption with a maximum at 274 nm. P15 exhibited a $[M+H]^+$ ion at m/z 537, suggesting it was hyperforin (**5**). P16 was identified as adhyperforin (**6**), based on the fragment ions at m/z 481, 469, 411 and 277 arising from loss of side chains. P13 and P14 contained an additional oxygen atom as compared to hyperforin (**5**). P11 and 12 exhibited UV spectra with maxima in the red-visible region suggesting these constituents were hypericin (**4**) derivatives. The TSP–MS conditions were not suitable for ionization of these two compounds; however, ESI in the negative ion mode exhibited a $[M-H]^-$ ion at m/z 519 and 503, confirming their identifications as pseudohypericin (**3**) and hypericin (**4**) respectively. Hypericin and its analogues do not readily form $[M+H]^+$ ions. Piperopoulos et al. also found that hypericin (**4**) and pseudohypericin (**3**) produce intense negative quasi-molecular ions by deprotonation provided a non-acidic eluent system is used (pH 7) [37]. Under neutral conditions the extent of deprotonation is sufficient to observe high intensities of $[M-H]^-$ ions. The characteristic MS–MS data of these compounds were also obtained by CID method [37].

2.4. Ginkgo: Ginkgo biloba (Ginkgoaceae)

Ginkgo is one of the most completely studied plants used in herbal medicine. A large number of polar and apolar compounds have been isolated from Ginkgo leaves. Extracts containing 24% total flavonoids and 6% terpene lactones produce effects on vascular and cerebral metabolic processes, and inhibit platelet-activating factor.

Terpene lactones have been identified in Ginkgo using HPLC–MS [8]. Gobbato et al. reported HPLC–TSP–MS analyses of its biflavones [38]. The biflavones (C–C dimeric flavonoids) from Ginkgo are derivatives of apigenin (Fig. 7). The four main constituents are: bilobetin (**2**), ginkgetin (**4**), isoginkgetin (**5**) and sciadopitysin (**6**). Two minor ones are amentoflavone (**1**) and sequojaflavone (**3**). Reversed-phase HPLC allowed for satisfactory separation of these six biflavones. Fig. 8 shows their HPLC–TSP–MS profiles (Fig. 8a) and UV trace at 330 nm (Fig. 8b). These structurally related biflavones have very similar UV spectra. MS information played a role in confirming their identification. A TSP interface was applied. However, an additional ionization source (filament-on mode) was used to provide maximum sensitivity, meaning a chemical ionization process is required to ionize these compounds. The protonated molecules $[M+H]^+$ appear as the base peak for these biflavones.

The MS response corresponding to the $[M+H]^+$ ions of the selected biflavones at m/z 539, 553, 567 and 581 is comparable with the UV response, but P1 and P3 did not have enough of a mass response. Their mass spectra were therefore obtained by injection of a more concentrated sample.

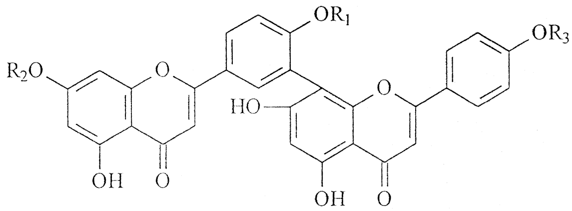

No.	Compound	R1	R2	R3	Mr
1	Amentoflavone	H	H	H	538
2	Bilobetin	Me	H	H	552
3	Sequojaflavone	H	Me	H	552
4	Ginkgetin	Me	Me	H	566
5	Isoginkgetin	Me	H	Me	566
6	Sciadopitysin	Me	Me	Me	580

Fig. 7. Structures of Ginkgo biflavones.

2.5. Tea: Camellia sinensis (Theaceae)

Tea is widely used as a daily beverage and has many beneficial pharmacological effects, considered to be primarily caused by tea flavanols (catechins) (Fig. 9). Dalluge et al. compared six reversed-phase

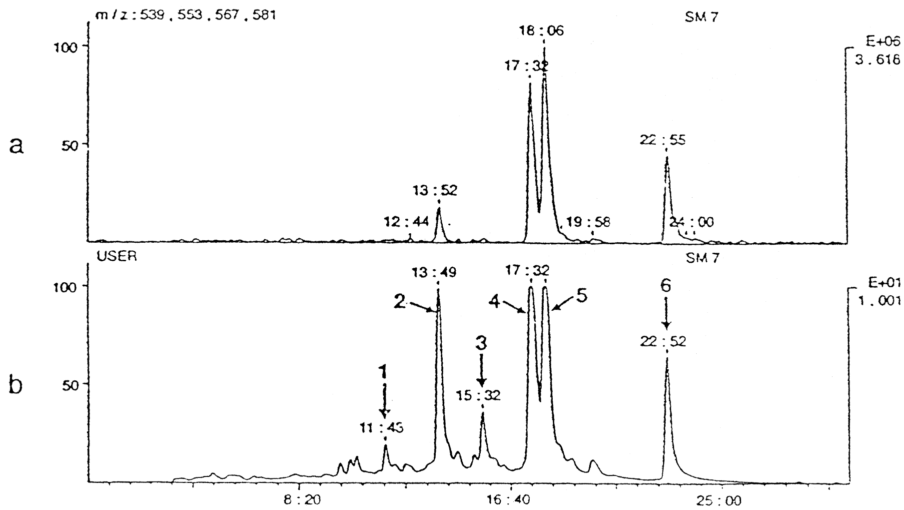

Fig. 8. HPLC–MS profile of purified Ginkgo biflavones. Time in min. (a) TSP-reconstructed ion chromatogram corresponding to $[M+H]^+$ ions at m/z 539, 553, 567 and 581. (b) UV trace at 330 nm. Peak identification: 1. amentoflavone; 2. bilobetin; 3. sequojaflavone; 4. ginkgetin; 5. isoginkgetin; 6. sciadopitysin. Reprinted with permission from Ref. [38].

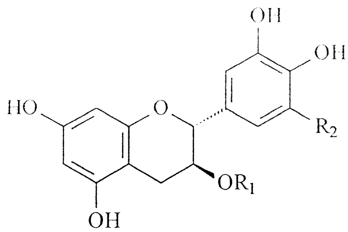

	R1	R2	Mr
(+)-Catechin (**C, 1**)	H	H	290

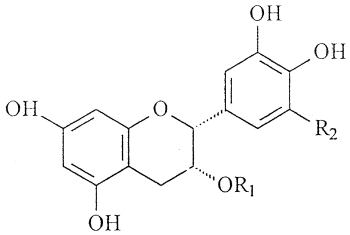

(-)-Epicatechin (**EC, 2**)	H	H	290
(-)-Epicatechin gallate (**ECg, 4**)	galloyl	H	442
(-)-Epigallocatechin (**EGC, 6**)	H	OH	306
(-)-Epigallocatechin gallate (**EGCg, 8**)	galloyl	OH	458

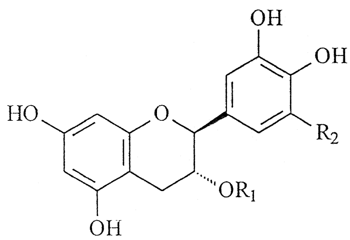

(-)-Catechin gallate (**Cg, 3**)	galloyl	H	442
(-)-Gallocatechin (**GC, 5**)	H	OH	306
(-)-Gallocatechin gallate (**GCg, 7**)	galloyl	OH	458

Fig. 9. Structures of tea catechins.

columns for the separation of tea catechins [39], and found that a monomeric C_{18} column significantly improved separation efficiencies. In particular, GCg (**7**) and C (**1**) can also be separated with this column. The use of an acidic mobile phase is essential for complete resolution of tea catechins.

Goto et al. separated eight tea catechins [plus GC (**5**) and Cg (**3**)] using a Develosil ODS-HG column and a water–MeCN–H_3PO_4 mobile phase. The linearity of the calibration curve was better at 231 nm than at 207 nm [40].

Lin et al. used LC–TSP–MS and CID spectra to study a tea catechins mixture [41]. The total ion chromatogram revealed only four distinct peaks. The mass spectra of the four peaks all gave abundant $[M+H]^+$ ions, consistent with the expected four major tea catechins: EC (**2**) at m/z 291, EGC (**6**) at m/z 307, ECg (**4**) at m/z 443 and EGCg (**8**) at m/z 459.

In addition to the $[M+H]^+$ ions, the presence of gallic esters in ECg (**4**) and EGCg (**8**) are indicated by the ions at m/z 275 and 291 derived from the loss of 168 amu from the two corresponding $[M+H]^+$ ions. By LC–PB–MS, two of the catechins, ECg (**4**) and EGCg (**8**), failed to give molecular ions, only fragmentation ions. CID spectra of the above $[M+H]^+$ ions reveal three types of cleavages, a, b and c, at the dihydropyran rings of the catechins, and elimination ions of the substituent at the 3-position of the ring (Fig. 10). The assignments can be made as follows: m/z 443 ($[MH^+]$), 291 ($[MH^+-R+H]$), 273 ($[MH^+-ROH]$), 165 ([cleavage b-R+H]), 153 ($[R^+]$), 151 ($[R^+$-2H]), 139 (cleavage a) and 123 (cleavage c).

Bailey et al. studied black tea liquor by LC–plasmaspray–MS [42]. In the plasmaspray interface, a voltage difference is applied between the capillary tube and the ion source block, producing a plasma from the HPLC eluent. Plasmaspray produces more fragmentation than TSP and ionizes a wide range of compounds. Bailey et al. also obtained TIC chromatograms for the aglycones of the main tea flavonoid glycosides (kaempferol and quercetin), 4-coumarylquinic acid and chlorogenic acid. No TIC chromatograms were obtained for myricetin or its glycosides, theogallin or theanine [42].

Kiehne et al. reported the analyses of flavanols, flavonol *O*-glycosides and flavone *C*-glycosides as well as caffeine, theobromine, theogallin, theanine and proanthocyanidins from tea by HPLC–TSP–MS [35,43,44]. All compounds are detected as pseudo-molecular ions $[M+H]^+$. The catechin gallates and flavonol glycosides are fragmented. This fragmentation due to the cleavage of esterified gallic acid is temperature dependent.

2.6. Soy: Glycine max (Leguminosae)

Soybeans contain three major isoflavones: daidzein, genistein and glycitein. These occur predominantly as glycosides (daidzin, genistin and glycitin),

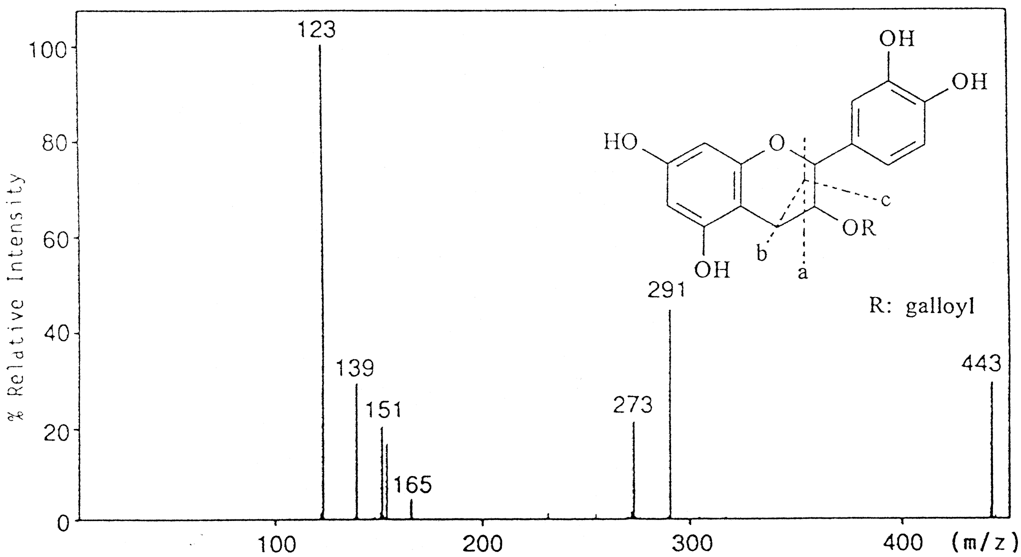

Fig. 10. CID spectrum for the $[M+H]^+$ at m/z 443 ion of ECg (**4**). Adapted from Ref. [41].

malonyl glucosides and minor acetyl glucosides. Daidzin, genistin and glycitin seem to have anticarcinogenic and estrogenic activities. Their aglycones daidzein and genistein have been in high concentrations in soy preparations.

Setchell et al. reported a simple isocratic reversed-phase system with MeOH–0.1 *M* NH_4OAc, pH 4.6 (60:40, v/v) as mobile phase on a Hypersil ODS column for separation of these isoflavonoids [45]. Using LC–TSP–MS, they optimized ionization conditions for mass spectral analysis of these isoflavonoids. Daidzein, genistein, formononetin, biochanin A and the cumarin coumestrol were all characterized by intense protonated molecular ions $[M+H]^+$ with no significant fragmentation. Barnes et al. identified isoflavone 6-*O*-MalGlc and 6-*O*-AcGlc conjugates in soy extracts using HPLC with a heated nebulizer (HN)-APCI and modified ESI-MS [46]. Using this system the isoflavone 6-*O*-AcGlc conjugate gave rise to the molecular ion $[M+H]^+$ and the $[M\text{-AcGlc}+H]^+$ ion. The isoflavone β-glucosides and 6-*O*-AcGlc conjugates yielded molecular ions in both positive and negative ion mass spectra, but the most abundant ion in each case corresponded to the aglycone. The intact $[M+H]^+$ molecular ion was the most abundant in mass spectra for each isoflavone 6-*O*-MalGlc in the ionspray interface with no heating. The other major ions were ammonium and potassium adducts and the aglycone ions $[M\text{-Mal-Glc}]^+$. Isoflavonoid acetate and malonates both occur in the same botanical extract due to decarboxylation of the malonate during work-up procedures, forming the acetate [47].

Simple phenolic acids are widespread in the hydrolyzed extracts of soybean leaves or roots. Moran et al. analyzed polyhydroxy phenolic acids and their glucosides from soybean nodules by HPLC, using an ion-exchange (Aminex) column [48]. This allowed for separation of β-hydroxybenzoic acid, vanillic acid and ten other phenolic acids. Both ESI and negative ion atmospheric pressure chemical ionization (APCI) interfaces were used. The pseudo-molecular ion $[M\text{-H}]^-$ was obtained for all compounds by ESI-MS and controlled fragmentation at 24 eV by tandem ESI–MS of the selected $[M\text{-H}]^-$ revealed the loss of a glycosidic moiety in all of the phenolic acids.

2.7. Kudzu: Pueraria lobata (Leguminosae)

Kudzu root is widely used in traditional Chinese medicine. Recently, its major constituents daidzin and daidzein were shown to suppress ethanol intake,

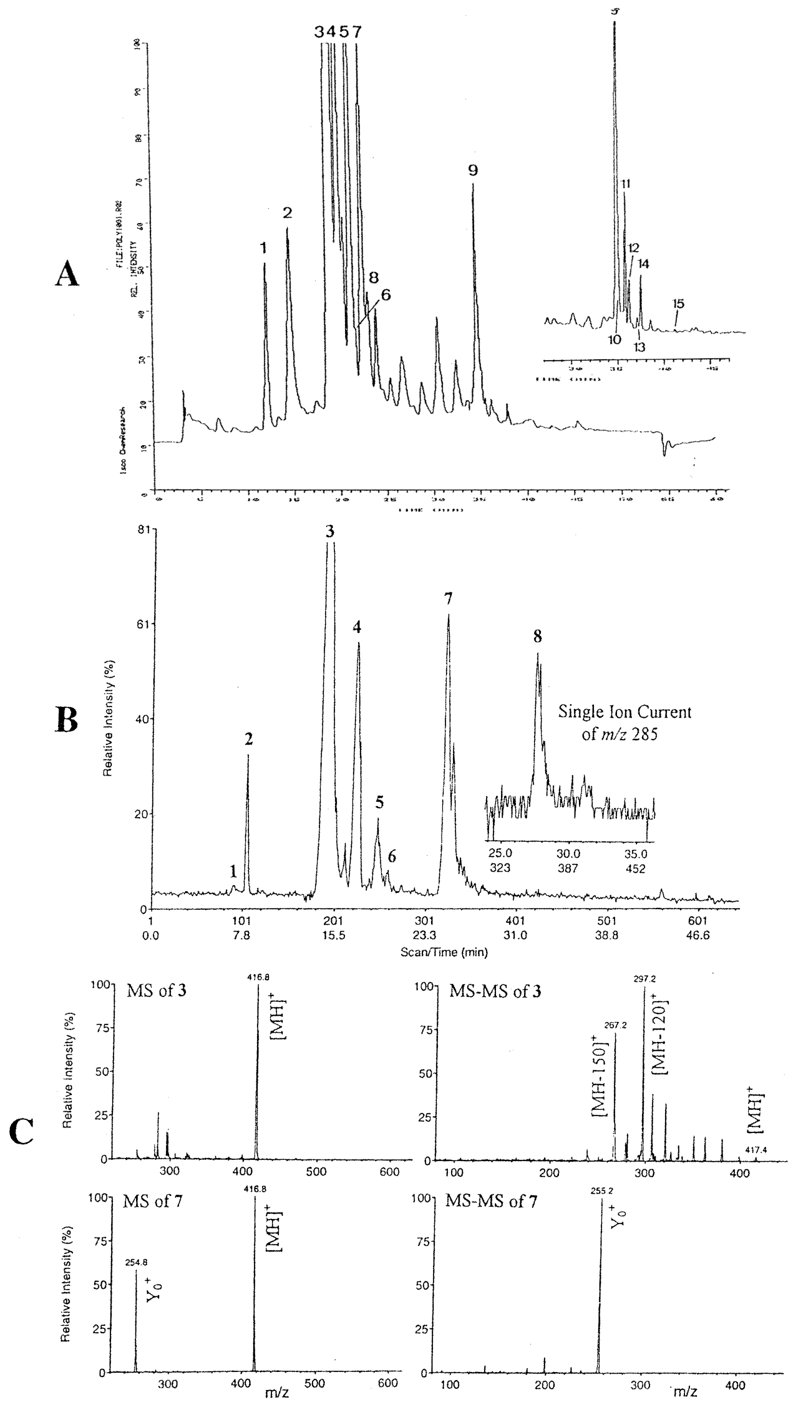

Fig. 11. (A) HPLC–UV chromatogram of a polyphenolic extract of kudzu and of the aglycone part (insert) of the acid hydrolysate (peak labels correspond to compound numbering). (B) HPLC–APCI–MS chromatogram of the glycoside fraction of kudzu extract. (C) MS–MS spectra of compounds **3** and **7**. Left panels: single APCI–MS spectra. Right panels: daughter ion mass spectra of selected $[M+H]^+$ ions on collisional activation recorded in the MS–MS mode. Reprinted with permission from Ref. [51].

thus offering promise as a safe and effective therapeutic agent against alcohol abuse [49,50].

Rong et al. have conducted full identification of the isoflavonoids in kudzu root by HPLC–DAD–MS using APCI or ESI in combination with CAD [51]. Fig. 11 shows a HPLC–UV and HPLC–APCI–MS(–MS) chromatogram of its extract. Fig. 12 shows the chemical structures of related compounds. The peak labels correspond to the compound numbers. The UV spectra of all the constituents, with the exception of compound **11**, exhibited absorption maxima in the range of 250–265 nm and around 300 nm. These features are typical of isoflavone glycosides. In the glycoside fraction, two major peaks (5 and 7) and two minor peaks (1 and 8) were no longer present following hydrolysis, suggesting that these compounds are *O*-glycosides. The first eluting peak in the aglycone fraction is compound **9**. Mass spectroscopy enables distinction between flavonoid *O*- and *C*-glycosides. The mass spectrum of an *O*-glycoside is generally characterized by an abundant fragment ion resulting from (terminal) glycosyl cleavage, as mentioned in the previous examples. In contrast, the aglycone moiety of *C*-glycosides is not produced. Thus, puerarin (**3**) (diadzein-8-*C*-D-glucoside, P3) and daidzin (**7**) (daidzein-7-*O*-D-glucoside, P7) can be readily distinguished.

Daidzin (**7**) showed a prominent fragment ion at m/z 255, due to loss of a β-glucose unit from $[M+H]^+$ at m/z 417. Puerarin (**3**), the most abundant constituent of kudzu (ca. 4% of the dry plant material) also gave $[M+H]^+$ at m/z 417, and an

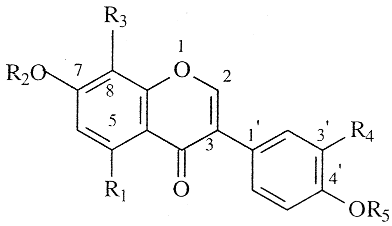

	R$_1$	**R$_2$**	**R$_3$**	**R$_4$**	**R$_5$**
Puerarin-4'-O-D-glucoside (**1**)	H	H	Glc	H	Glc
3'-Hydroxypuerarin (**2a**)	H	H	Glc	OH	H
3'-Hydroxypuerarin-4'-O-deoxyhexoside (**2b**)	H	H	Glc	OH	deoxyl-hexosyl
Puerarin (**3**)	H	H	Glc	H	H
3'-Methoxypuerarin (**4**)	H	H	Glc	OMe	H
6''-O-D-Xylosylpuerarin (**5**)	H	H	Glc^6-Xyl	H	H
3'-Methoxy-6''-O-D-xylosyl-puerarin (**6**)	H	H	Glc^6-Xyl	OMe	H
Daidzin (**7**)	H	Glc	H	H	H
3'-Methoxydaidzin (**8**)	H	Glc	H	OMe	H
Daidzein (**9**)	H	H	H	H	H
3'-Methoxydaidzein (**10**)	H	H	H	OMe	H
Genistein (**12**)	OH	H	H	H	H
Daidzein-7-O-methyl ether (**13a**)	H	Me	H	H	H
3'-Methoxydaidzein-7-O-methyl ether or	H	Me	H	OMe	H
3'-Methoxyformononetin (**13b**)	H	H	H	OMe	Me
Formononetin (**14**)	H	H	H	H	Me
Biochanin A (**15**)	OH	H	H	H	Me

Fig. 12. Structures of kudzu flavonoids.

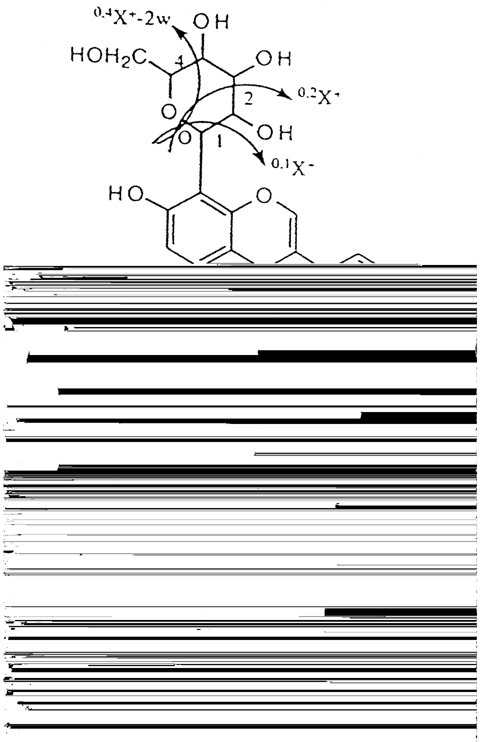

Fig. 13. Mass fragmentations in purarin (**3**) and daidzin (**7**). Reprinted with permission from Ref. [51].

important fragment ion at m/z 297 by loss of 120 amu. Typical fragment ions of *C*-glucosides are $[MH\text{-}120]^+$ and $[MH\text{-}150]^+$. Fig. 13 shows the most prominent mass fragmentations in daidzin (**7**) and puerarin (**3**).

2.8. Astragalus: Astragalus membranaceus and A. mongholicus (Leguminosae)

Astragalus is a well-known tonic used in traditional Chinese medicine to reinforce 'Qi' (vital energy). Positive effects reported from twentieth-century research include enhanced immunostimulatory and macrophage activities. Its main active constituents are triterpene saponins, flavonoids and polysaccharides.

Lin et al. have identified the eight major flavonoids in astragalus using HPLC–ESI–MS in our laboratory [52], based on the comparison with authentic standards. Fig. 14 shows the HPLC–UV chromatogram of its extract. Fig. 15 shows the chemical structures of some flavonoids in astragalus. These compounds are calycosin-7-*O*-β-D-glucoside (**2**, P1), calycosin-7-*O*-β-D-glucoside-6″-*O*-malonate (**3**, P3), ononin (P5), (6aR, 11aR)-3-hydroxy-9,10-dimethoxypterocarpan-3-*O*-β-D-glucoside (**5**, P6),

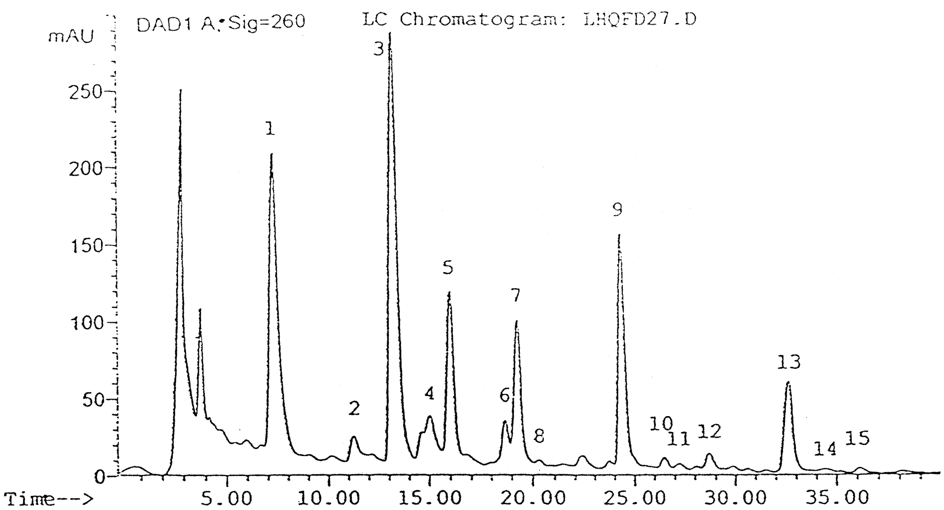

Fig. 14. HPLC–UV chromatogram of the extract of Astragalus. Time in min. Adapted from Ref. [52].

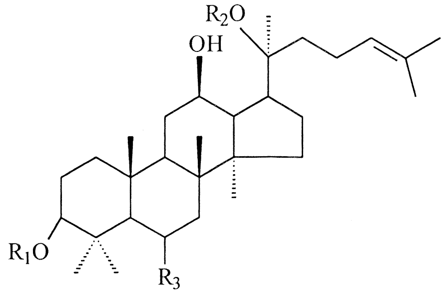

Ginsenosides	R1	R2	R3	Mr
Rb1	-Glc^2-Glc	-Glc^6-Glc	H	1108
Rb2	-Glc^2-Glc	-Glc^6-Ara(p)	H	1078
Rc	-Glc^2-Glc	-Glc^6-Ara(f)	H	1078
Rd	-Glc^2-Glc	-Glc	H	946
Re	H	-Glc	-O-Glc^2-Rha	946

Glc: glucose; Ara(p): arabinose in pyranose form; Ara(f): arabinose in furanose form; Rha: rhamnose.

A

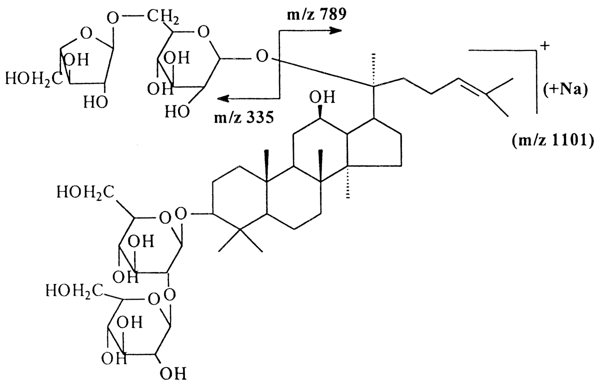

B

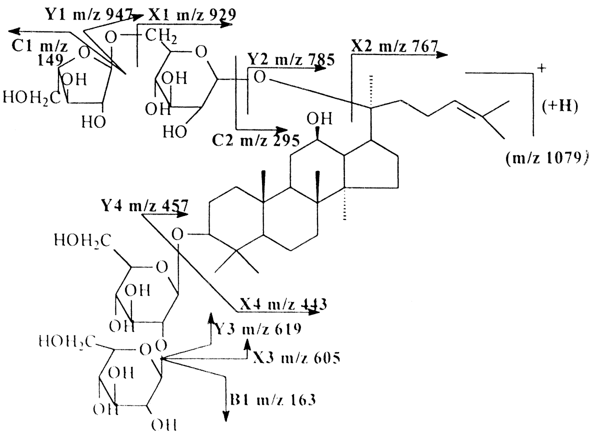

Fig. 18. Chemical structure of ginsenosides and MS fragmentation patterns of ginsenoside Rc obtained from CID spectra of $[M+Na]^+$ (a) and $[M+H]^+$ (b). Adapted from Ref. [56].

corresponding to the loss of the glycosidic portion from the $[M+Na]^+$ adduct, and the ion at m/z 588 (deacetylated sapogenin) is also present. These two peaks are identified as compounds **1** and **2** respectively. All of the other peaks were identified in the same way and showed intense adduct ions as $[M+Na]^+$ and $[M-H_2O+MeCN+Na]^+$.

3.2. Ginseng: Panax ginseng and P. quinquefolius (Araliaceae)

Ginseng is used in Chinese herbal medicine as a rejuvenating tonic. *Panax ginseng* is commonly known as Chinese or Korean ginseng and *P. quinquefolius* as American ginseng. Ginsenosides are the major active constituents (Fig. 18).

Wang et al. used HPLC–ESI–MS–MS for characterization and quantification of the ginsenosides in extracts of both American and Chinese ginseng root [56]. The $[M+H]^+$ and $[M+Na]^+$ ions were observed for ginsenoside standards (Rb1, Rb2, Rc, Rd, Re, Rf and Rg1). The glycosidic linkage, the core and the attached sugars of the ginsenosides can be determined from CID spectra of the protonated parent ion.

Fig. 18 (a and b) shows MS fragmentation patterns obtained from CID spectra of $[M+Na]^+$ and $[M+H]^+$ of ginsenoside Rc, respectively. The CID spectra of ginsenosides show large differences between the protonated and sodiated species. The sodiated species produced only one glycosidic bond cleavage and gave limited structural information. For example, the expected fragment ion arising from loss of the terminal glucose (-R_2) from Rb1, Rb2, Rc and Rd was observed at m/z 789 (Fig. 18a). More structural information can be obtained from the CID spectra of protonated molecules (Fig. 18b) than sodiated species.

Breemen et al. used an aminopropyl silica HPLC column followed by on-line ESI–MS detection to analyze ginseng saponins [57]. Ginsenosides eluted in order of increasing molecular weight and were detected as $[M+Na]^+$ or $[M+138]^+$ adducts. The cation at m/z 138 was identified as (3-ammonium propyl) trihydroxysilane $^+NH_4(CH_2)_3Si(OH)_3$, which was either a byproduct of the stationary phase synthesis or a stationary phase degradation product.

3.3. Aridan: Tetrapleura tetraptera (Leguminosae)

This West African tree is known locally as Aridan and is traditionally used for the treatment of rheumatic pains. Five saponins (**1**–**5**) were isolated and found to be powerful natural molluscacides [58] (Fig. 19).

HPLC analysis of the crude methanolic extract of its fruit showed six major peaks. Post-column addition of a 0.5 *M* NH_4OAc was used to provide a volatile buffer for ion evaporation ionization. The TSP mass spectra of saponins **1**, **2**, **4** and **5** displayed strong $[M+H]^+$ quasi-molecular peaks, together with adduct species such as $[M+MeCN+NH_4]^+$, confirming their molecular masses. In addition, an important $[A+H]^+$ peak for the aglycone was visible in these spectra.

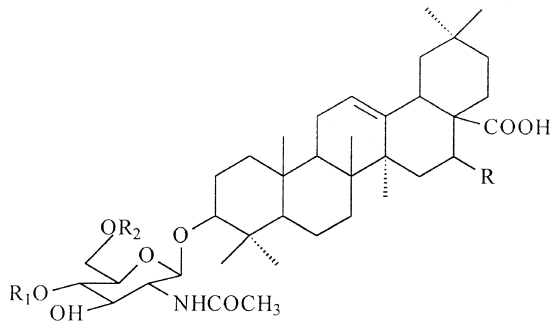

1	R=R1=R2=H	Mr 659
2	R=α-OH, R1=R2=H	Mr 675
4	R=H, R1=Gal, R2=H	Mr 821
5	R=R1=H, R2=Glc	Mr 821

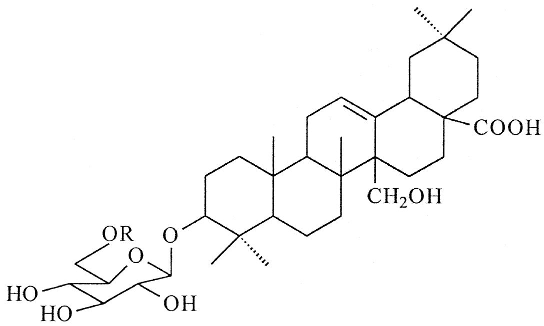

3 R=Glc Mr 796

Fig. 19. Chemical structures of saponins (**1**–**5**) from Aridan.

The mass spectrum of saponin **3** revealed a different pattern. Small quasi-molecular peaks at m/z 855 $[M+MeCN+NH_4]^+$, 814 $[M+NH_4]^+$ and 797 $[M+H]^+$ confirmed the molecular mass. The base peak at m/z 784 $[(M+NH_4)\text{-}30]^+$ resulted from rapid elimination of a CHOH fragment. A small peak resulting from the loss of one sugar was present at m/z 622 $[784\text{-hexose}]^+$.

The authors also reported the mass spectrum of a saponin triglycoside isolated from another African plant (Fig. 20). A TSP mass spectrum showed a $[M+NH_4]^+$ quasi-molecular peak. Subsequent losses of sugars were observed. Loss of a rhamnosyl $[(M+NH_4)\text{-}146]^+$ moiety and a glucosyl $[(M+NH_4)\text{-}162]^+$ moiety indicated that both sugars were in terminal positions. Additional signals were observed at m/z 650, 636 and 474, and corresponded to elimination of both sugar moieties along with an additional inner glucuronic acid residue. The fragmentation patterns clearly indicated that rhamnose was attached to glucuronic acid and that glucose belonged to a second chain.

3.4. Tribuli: Tribulus terrestris (Zygophyllaceae)

Tribuli fruit is a traditional Chinese herb widely used for the treatment of liver and eye diseases. A number of steroidal saponins have been isolated from tribuli fruit. Fang et al. have separated a chromatographic fraction composed mainly of steroidal saponins. They analyzed this fraction by ESI–MS with sequential MS (ESI–MS^n) [59].

The full-scan ESI mass spectrum of its steroidal saponin mixture is shown in Fig. 21. All of the major peaks were $[M+Na]^+$ adducts and six saponins can be assumed from the molecular mass of these compounds. **A**, **B**, **C**, **D**, **E** and **H** correspond to terrestrosin C ($M_r=916$), terrestrosin E ($M_r=918$), desgalactotigonin or gitonin ($M_r=1034$), terrestrosin ($M_r=1048$), F-gitonin or desglucolanatigonin II ($M_r=1050$) and tribulosin ($M_r=1150$), respectively. Compounds **F**, **G**, and **I** are probably three unknown steroidal saponins.

All of these saponins displayed similar fragmentation behavior in ESI–MS^n. A characteristic cross-

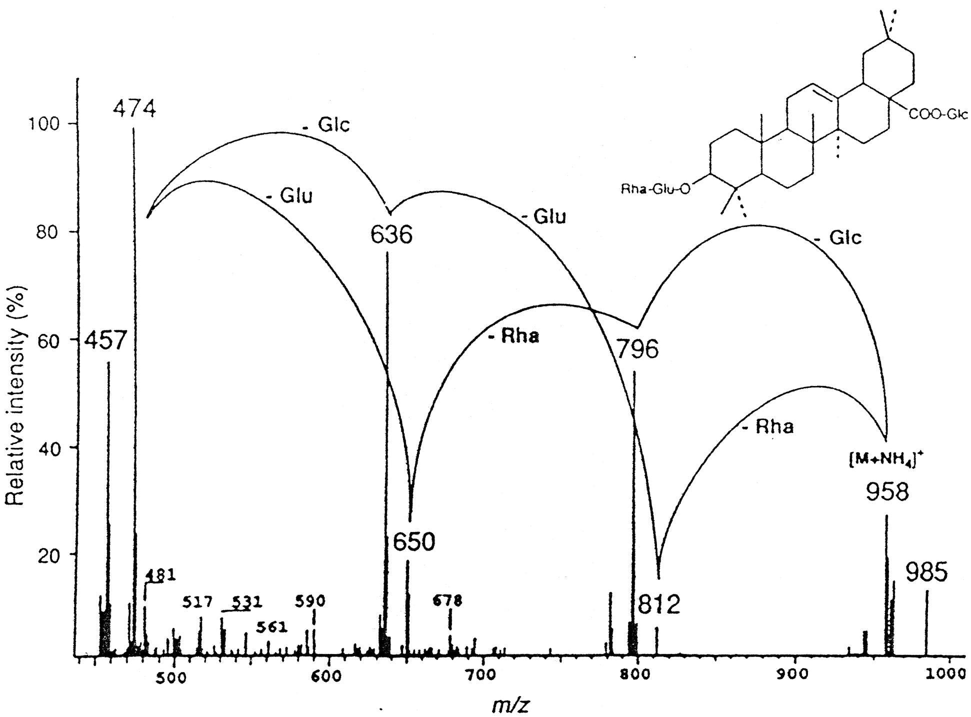

Fig. 20. TSP mass spectrum of saponin triglycoside obtained in the flow-injection mode. Adapted from Ref. [58].

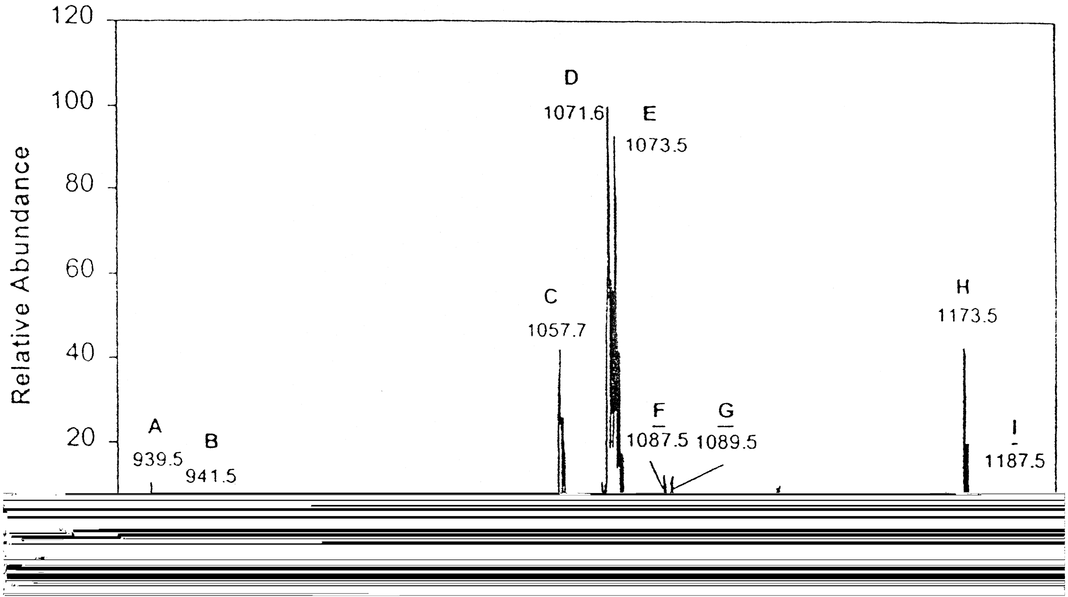

Fig. 21. Full-scan mass spectrum of the steroidal saponin mixture of fraction four from tribuli fruit. Reprinted with permission from Ref. [59].

ring cleavage pattern could be used as a fingerprint for their identification. Fig. 22 is a MS–MS spectrum of sodium cationized saponin **D**. The MS–MS of the sodium adduct of **D** afforded two intense fragment ions at *m/z* 909 and 939. The mass differences between them and the precursor ion at *m/z* 1071 were 162 and 132 Da, indicating loss of either a glucose unit or a xylose unit respectively. The ions at *m/z* 641 and 659 were clue to loss of an aglycone unit or a deoxyaglycone unit respectively.

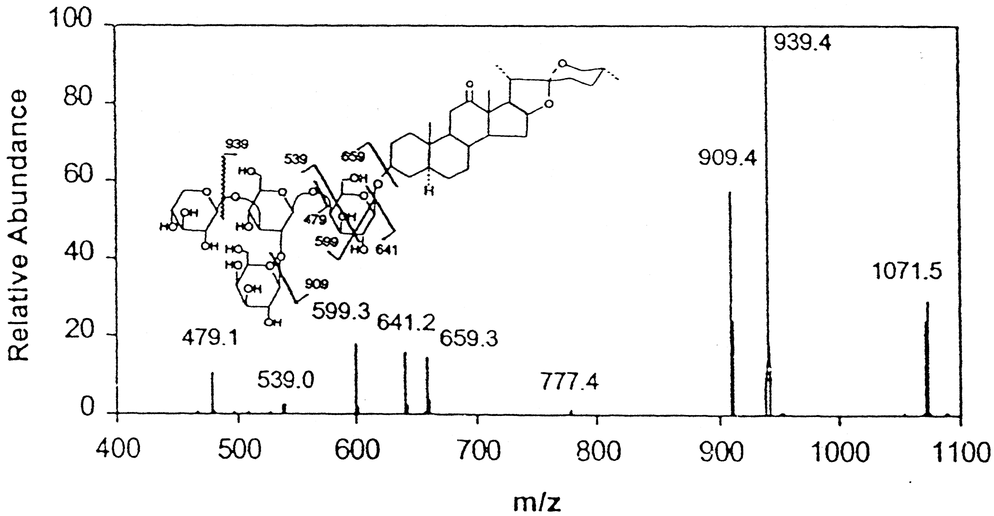

Fig. 22. MS–MS spectrum of sodium cationized saponin D from tribuli fruit. Reprinted with permission from Ref. [59].

secondary hydroxyl group, exhibited [M-HCHO-CH_3]$^+$ as the base peak.

Compounds with a two methoxyl group at C-9 and C-10 of the isoquinoline ring (**1**, **2**, **5**, **6** and **7**) all exhibited a fragment ion at m/z [M-HCHO]$^+$.

4.2. Australian Moreton Bay Chestnut: Castanospermum australe (Leguminosae)

Chen et al. analyzed polyhydroxylated alkaloids from the seeds of *Castanospermum australe* [61]. These alkaloids have potent inhibitory effects on a variety of enzymes and on the growth of HIV and tumor cells. These alkaloids lack a chromophore in the structure, making them very difficult to detect with common photometric detection. Use of a HPLC–TSP–MS method should be appropriate, because the alkaloids have the high proton affinity characteristic of nitrogen-containing compounds.

Chen et al. used a cation-exchange column to

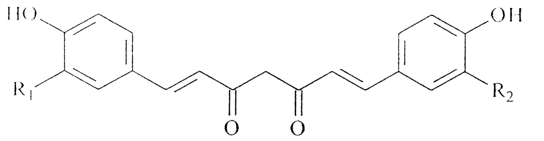

Curcumin (**1**)	R1=R2=OMe	Mr 368
Demethoxycurcumin (**2**)	R1=OMe, R2=H	Mr 338
Bisdemethoxycurcumin (**3**)	R1=R2=H	Mr 308

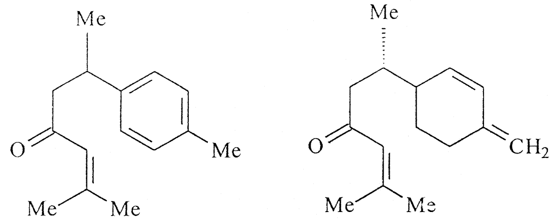

ar-Turmerone (**4**) Mr 216 Curlone (**5**) Mr 218

Fig. 25. The structures of chemical constituents in turmeric.

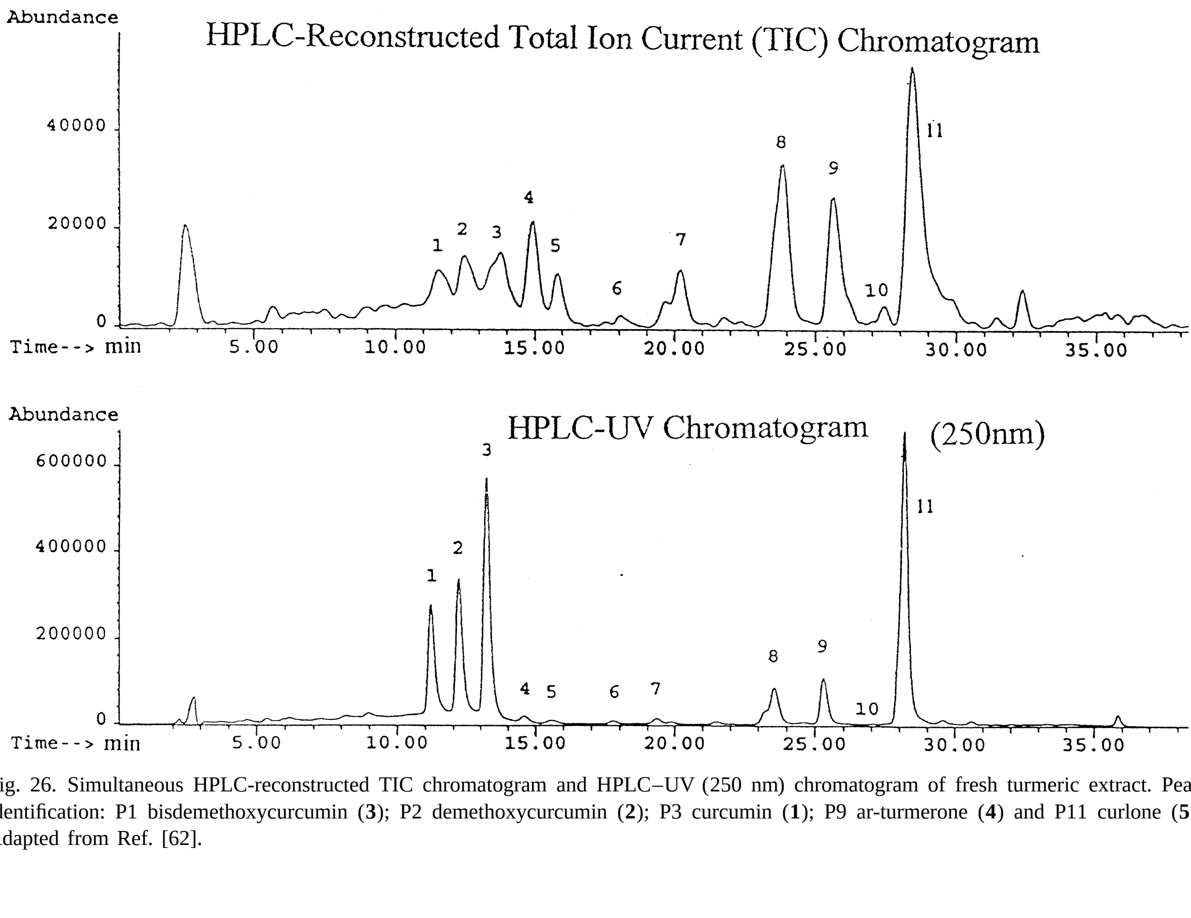

Fig. 26. Simultaneous HPLC-reconstructed TIC chromatogram and HPLC–UV (250 nm) chromatogram of fresh turmeric extract. Peak identification: P1 bisdemethoxycurcumin (**3**); P2 demethoxycurcumin (**2**); P3 curcumin (**1**); P9 ar-turmerone (**4**) and P11 curlone (**5**). Adapted from Ref. [62].

analyze different extraction fractions, with MeCN–water (5:95) containing 0.015 *M* of $HCOONH_4$ as mobile phase. Ammonium in the mobile phase was used to generate TSP ionization. The major peaks $[M+H]^+$ at *m/z* 190 were identified as castanospermine (**1**), 6-epi-castanospermine (**2**) and australine (**3**), based on comparison of retention times with authentic compounds (Fig. 24).

5. Miscellaneous natural products

Many other types of natural products can be ionized using ESI–MS. Some of these compounds, such as kavalactones and gingerols, can also be regarded as phenolics based on their biosynthesis. They are described in this section, due to their diverse structures and strong ionization behavior in ESI interface.

5.1. Turmeric: Curcuma longa (Zingiberaceae)

Turmeric is a major component of curry powder. It is well known for its coloring, flavoring and digestive properties. Three major yellow pigments in turmeric are diarylheptane derivatives. They are curcumin (**1**), demethoxycurcumin (**2**) and bis-demethoxycurcumin (**3**) (Fig. 25). The major constituents of turmeric volatile oil are bisabolane sesquiterpenes.

Both the HPLC–MS and HPLC–UV (250 nm) chromatogram of a fresh turmeric extract are shown in Fig. 26 [62]. P3, 2 and 1 had similar UV spectra, characteristic of curcuminoids with λ_{max} at 425 nm. They all showed intense protonated molecules $[M+H]^+$ at *m/z* 369, 339 and 309, less intense adduct ions $[M+Na]^+$ at *m/z* 391, 361 and 331 and sodiated dimer ions $[2M+Na]^+$ at *m/z* 759, 699 and 639 respectively. They were identified as compounds **1**, **2**, and **3**, based on these data and comparison with the standard compounds.

The identities of P9 and 11 as ar-turmerone (**4**) and curlone (**5**) were confirmed by comparing their UV and MS data to the isolated pure compounds that were structurally confirmed by ^{1}H-NMR in our laboratory. P9 showed an intense protonated molecule $[M+H]^+$ at *m/z* 217 and an adduct ion $[M+Na]^+$ at *m/z* 239. P11 showed an intense protonated molecule $[M+H]^+$ at *m/z* 219 and an adduct ion $[M+Na]^+$ at *m/z* 241.

P4, P6 and P8–10 were identified in the same way. Not only individual curcuminoids, but also a number of major essential oil constituents, could be identified from a single HPLC run. The method provides a reliable fingerprint for turmeric, distinguishing it from other *Curcuma* species.

Hiserodt et al. reported characterization of powdered turmeric by HPLC–TSP–MS and HPLC–PB–MS [63]. Three curcuminoids, ar-tumerone and curlone were identified based on PB-MS fragmentation data. The volatile and some semi-volatile compounds are not readily analyzed by HPLC–PB–MS because they may be lost in the membrane separator used to remove solvents, so these were identified by GC–MS [63].

5.2. Saffron: Crocus sativus (Iridaceae)

The dried intact stigmas of saffron are widely used

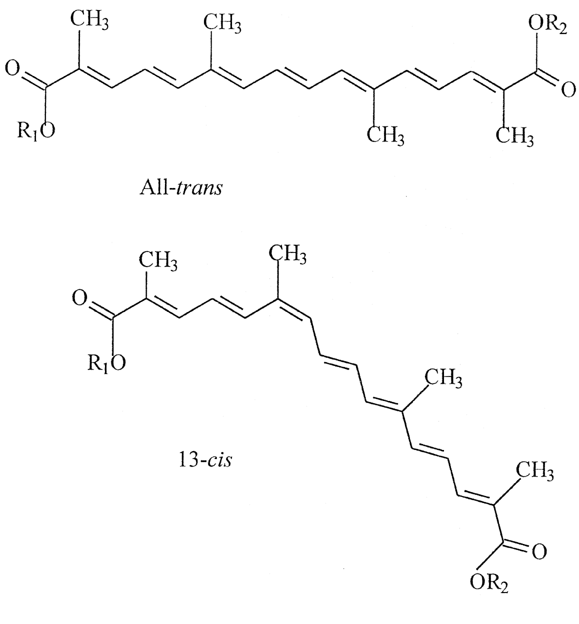

Crocin-4 (**1**) R1=R2=β-D-gentiobiosyl Mr 976
Crocin-5 (**2**) R1=Three β-D-glucosyl (Z)
R2=β-D-gentiobiosyl (X) Mr 1138

Fig. 27. Chemical structures of crocin-4 and crocin-5 from saffron.

as a condiment and food additive. In Chinese herbal medicine, saffron stigmas are occasionally used to treat painful chest and menstruation obstructions. The major compounds are *cis*- and *trans*-crociris, which are glucosyl esters of 8,8′-diapcarotene-8, 8′-dioic acid (crocetin) (Fig. 27). Only a few groups of carotenoids, such as crocins, are water-soluble.

Tarantilis et al. determined saffron components in crude plant extract using HPLC–DAD–ESI–MS [64]. Fig. 28 is a total ion chromatogram of a MeOH–water (50:50) extract of saffron. Carotenoids have characteristic spectra in the visible region with double peaks between 400 and 500 nm, and in the UV region between 320 and 340 nm.

The *cis–trans* isomers of crocins were identified with the aid of DAD. Crocins-4 (**1**) (*cis* and *trans*), the major components, were assigned as P10 and P5. Its precursor, crocetin, was esterified with one gentiobiose (Gnt = β-D-glc-1→6-β-D-glc) at each end. It gave an ion at m/z 999 $[M+Na]^+$. Elimination of a terminal gentiobiosyl group was observed, generating peaks at m/z 675 $[(M+Na+H)\text{-Gnt}]^+$ and 329 $[\{(M+Na+H)\text{-Gnt}\}\text{-Gnt}]^+$. An additional ion $[M+2Na]^+/2$ at m/z 511 was also observed.

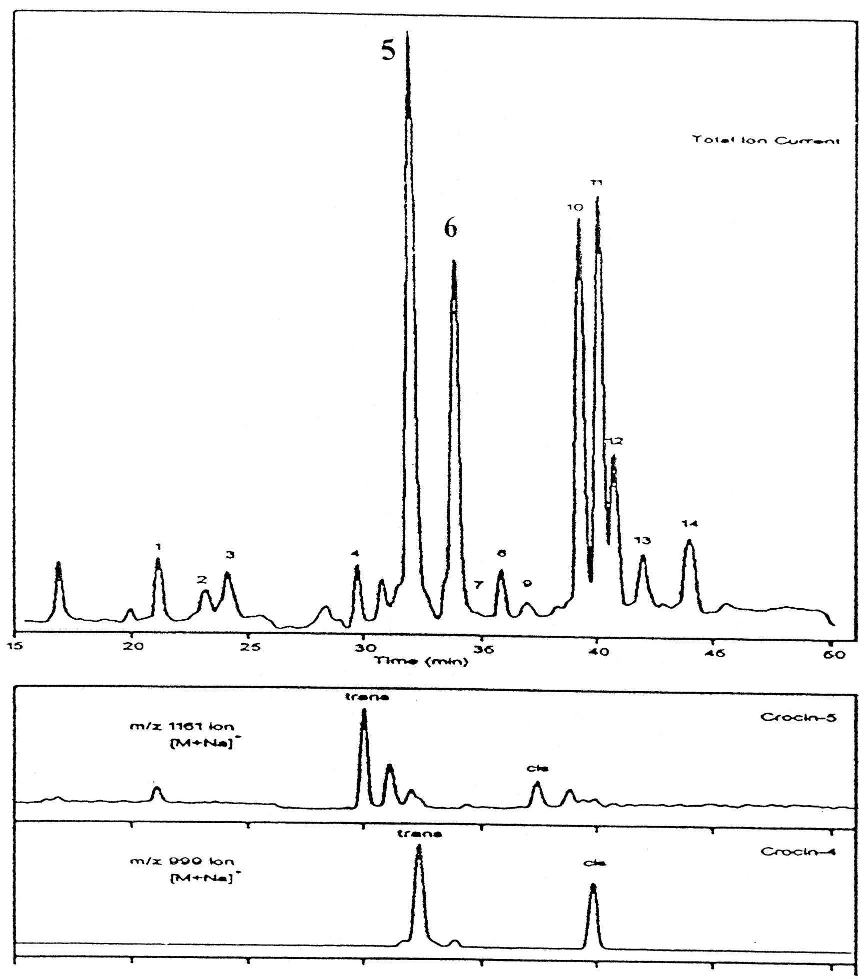

Fig. 28. Total ion chromatogram and selected-ion chromatogram for the HPLC–ESI–MS analysis of MeOH–water (50:50) extract of saffron. P10 and 5: crocin-4 (**1**) (*cis* and *trans*); P9 and 4: crocin-5 (**2**) (*cis* and *trans*). Adapted from Ref. [64].

Minor amounts of crocetin pentaglucosylates crocins-5 (**2**) (*cis* and *trans*) were detected (P9 and P4). Crocins-5 (**2**) displayed an ion at m/z 1161 $[M+Na]^+$. Additional signals were observed at m/z 837 $[(M+Na)\text{-Gnt}]^+$, 797 $[M\text{-Gnt}]^+$ and 592 $[M+2Na]^+/2$.

A simple HPLC–UV method for simultaneously quantifying crocins 1–4 and crocetin in saffron has been published [65].

5.3. Echinacea: Echinacea angustfolia, E. purpurea and E. pallida (Compositae/Asteraceae)

Herbal medicines from the genus *Echinacea* are the most widely used herbal remedies in Europe and the United States.

Alkamides are one of the classes of compounds in echinacea which exhibit immunostimulatory activities. He et al. have identified nine alkamides in the root of *E. purpurea* using HPLC–DAD–ESI–MS [66]. All alkamides gave intense $[M+H]^+$ and sodiated dimer ions in the TIC chromatogram. The primary alkamide in echinacea is the isomeric pair dodeca-2*E*,4*E*,8*Z*,10*E*/*Z*-tetraenoic acid isobutylamide. Fig. 29 shows its chemical structure and mass spectrum.

5.4. Ginger: Zingiber officinale (Zingiberaceae)

The constituents responsible for the pungent taste of ginger are a homologous series of phenolic ketones known as (4)-, (6)-, (8)-, (10)- and (12)-gingerols (Fig. 30). The shogaol series of compounds, even more pungent than the gingerols, is virtually absent from fresh ginger, and is derived from the corresponding gingerols during thermal processing or long-term storage. He et al. have analyzed fresh ginger and oleoresin extracts of ginger by HPLC–DAD–ESI–MS [67]. The highest ion signal intensity $[M+Na]^+$ was observed for (6)-, (8)-, and (10)-gingerols, while the highest ion signal intensity $[M+H]^+$ was observed for (6)-, (8)-, and (10)- shogaol. The (6)-, (8)- and (10)- gingerols and (6)- and (8)- shogaols also formed sodiated dimer

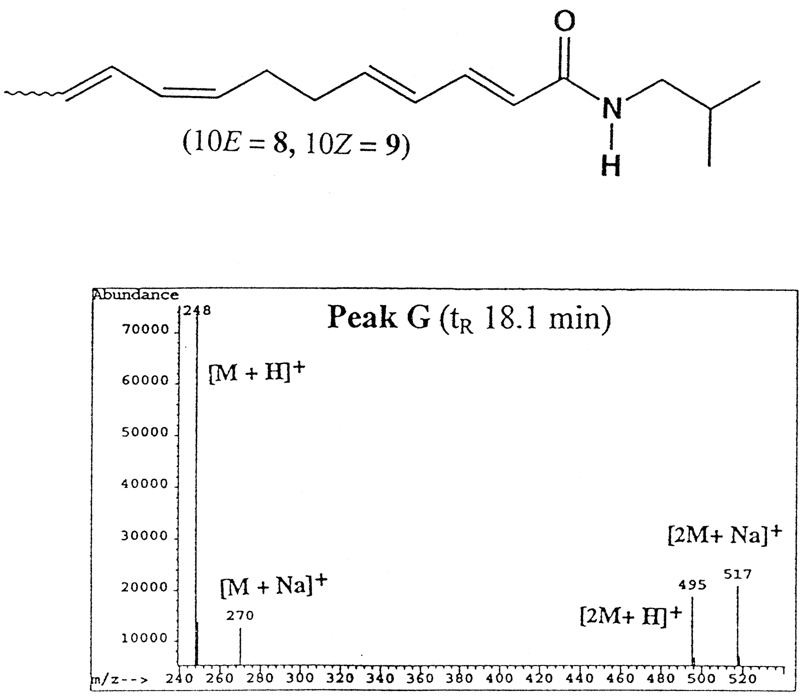

Fig. 29. The structure of the isomeric pair of dodeca-2*E*,4*E*,8*Z*,10*E*/*Z*-tetraenoic acid isobutylamide (M_r 247) and its mass spectrum. Adapted from Ref. [66].

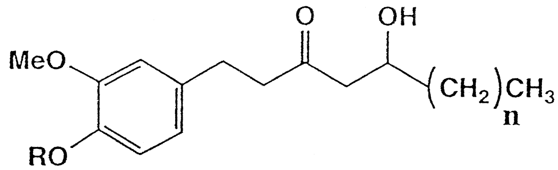

Compound	n	R	Mr
[4]-gingerol	2	H	266
[6]-gingerol	4	H	294
[8]-gingerol	6	H	322
[10]-gingerol	8	H	350
[12]-gingediol	10	H	380

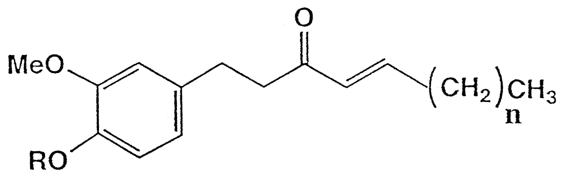

Compound	n	R	Mr
[6]-shogaol	4	H	276
[8]-shogaol	6	H	304
[10]-shogaol	8	H	332

Fig. 30. Chemical structures of gingerols and shogaols in ginger.

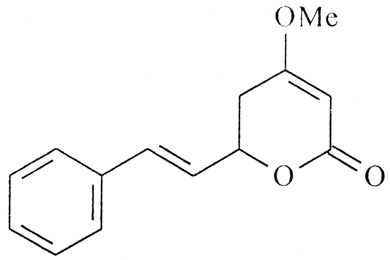

Kavain (**1**) Mr 230

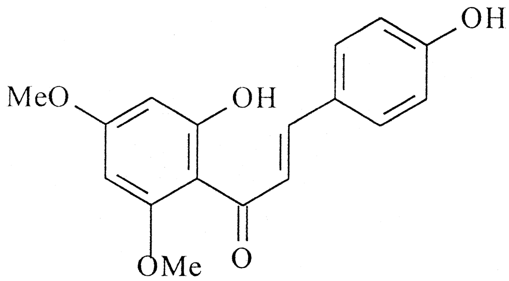

Flavokavain C (**2**) Mr 300

Fig. 31. Chemical structures of kavain (**1**) and flavokavain C (**2**).

ions. These compounds have molecular masses different from one another by 28 Da, making identification more confident.

5.5. Kava: Piper methysticum (Piperaceae)

Fresh or dried kava roots have been traditionally prepared as a beverage in most of the Pacific islands, used in social rituals as well as for soothing the nerves and inducing relaxation. The main active compounds of kava root are kavalactones. Fig. 31 gives the chemical structures of its two constituents kavain (**1**) and flavokavain C (**2**). HPLC–DAD–ESI–MS was used to study the chloroform extract of kava in our laboratory [68]. Thirteen kavalactones and flavokavains were identified and all showed very intense molecular ions $[M+H]^+$ and adduct ions except flavokavain C (**2**), which showed an intense negative ion $[M\text{-}H]^-$ at m/z 299.

Shao et al. reported that six major kavalactones can be completely separated by YM S-5 column; six kavalactones were confirmed by LC–APCI–MS analysis operating in the positive ion mode [69].

5.6. Schisandra: Schisandra chinensis and S. spenanthera (Magnoliaceae)

The fruit of *Schisandra* is a famous traditional Chinese medicine used as a tonic and sedative. The lignan group, a phenylpropanoid dimer linked by oxidative coupling (8–8′ bond), represents its active compounds.

The content and distribution of lignans is extremely varied in different *Schisandra* species (25 species worldwide). A HPLC chromatogram should provide a reliable fingerprint that can be used to distinguish different species, thus peak identification is very necessary. He et al. have unambiguously identified six major lignans in the fruit extract of *S. chinesis* by HPLC–DAD–ESI–MS [70]. Their identification was confirmed by comparison with the authentic compounds schisandrin (**1**), schisanhenol (**2**), deoxyschisandrin (**3**), γ-schisandrin (**4**), and schisan-

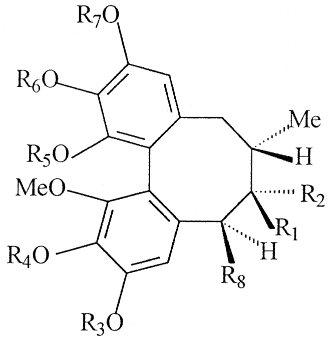

Compound	R1	R2	R3	R4	R5	R6	R7	R8	Mr
Schisandrin (**1**)	OH	Me	Me	Me	Me	Me	Me	H	432
Schisanhenol (**2**)	H	Me	Me	Me	H	Me	Me	H	402
Deoxyschisandrin (**3**)	H	Me	Me	Me	Me	Me	Me	H	416

Fig. 32. Chemical structures of lignan compounds in Schisandra.

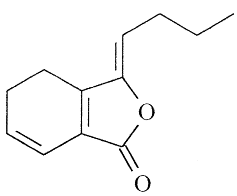

Z-Ligustilide (**1**)

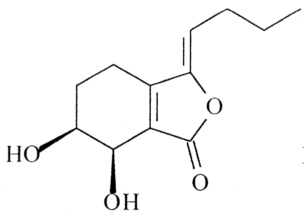

Senkyunolide H (**4**)

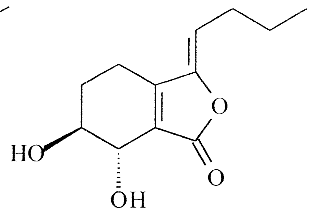

Senkyunolide I (**5**)

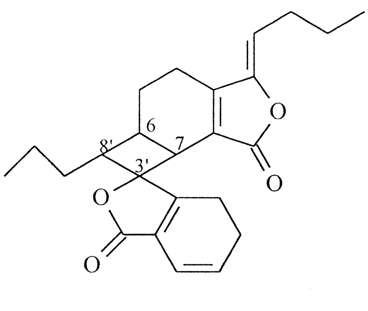

Z,Z'-6,8',7,3'-Diligustilide (**2**)

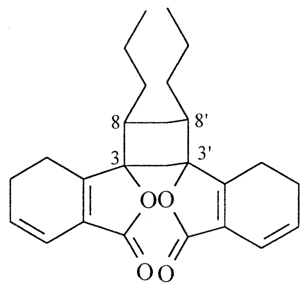

Z,Z'-3,3',8,8'-Diligustilide (**3**)

Fig. 33. *Z*-ligustilide (**1**) and its oxidation products in Dong Quai.

[11] J.L. Wolfender, K. Hostettmann, in: J.T. Arnason, R. Mata, J.T. Romeo (Eds.), Phytochemistry of Medicinal Plants, Recent Advances in Phytochemistry, Vol. 29, Plenum Press, New York, 1995, p. 189.
[12] S. Zhou, M. Hamburger, J. Chromatogr. A 755 (1996) 189.
[13] J.L. Wolfender, S. Rodriguez, K. Hostettmann, J. Chromatogr. A 794 (1998) 299.
[14] M. Careri, A. Mangia, M. Musci, J. Chromatogr. A 794 (1998) 263.
[15] M.T. Huang, C.T. Ho, C.Y. Lee (Eds.), Phenolic Compounds in Food and Their Effects On Health II, Antioxidants and Prevention, ACS Symposium Series, Vol. No. 507, ACS, Washington, DC, 1992.
[16] J.L. Wolfender, K. Hostettmann, J. Chromatogr. 647 (1993) 191.
[17] P. Pietta, R.M. Facino, M. Carini, P. Manri, J. Chromatogr. A 661 (1994) 121.
[18] A. Baldi, R.T. Rosen, E.K. Fukuda, C.T. Ho, J. Chromatogr. A 718 (1995) 89.
[19] G. Rath, A. Tonre, M. Nianga, J.L. Wolfender, K. Hostettmann, Chromatographia 41 (1995) 332.
[20] L.W. Sumner, N.L. Paiva, R.A. Dixon, P.W. Geno, J. Mass Spectrom. 31 (1996) 472.
[21] A. Raffaelli, G. Moneti, V. Mercati, E. Toja, J. Chromatogr. A 777 (1997) 223.
[22] H.L. Constant, K. Slowing, J.G. Graham, J.M. Pezzuto, G.A. Cordell, C.W.W. Beecher, Phytochem. Anal. 8 (1997) 176.
[23] S. Hakkinen, S. Auriola, J. Chromatogr. A 829 (1998) 91.
[24] U. Justesen, P. Knuthsen, T. Leth, J. Chromatogr. A 799 (1998) 101.
[25] J.F. Stevens, A.W. Taylor, M.L. Deinzer, J. Chromatogr. A 832 (1999) 97.
[26] D. Ryan, K. Robards, S. Lavee, J. Chromatogr. A 832 (1999) 87.
[27] M.M. Nindi, B.V. Kgarebe, J.L. Wolfender, B.M. Abegaz, Phytochem. Anal. 10 (1999) 69.
[28] J.F. Hammerstone, S.A. Lazarus, A.E. Mitchell, R. Rucker, H.H. Schmitz, J. Agric. Food. Chem. 47 (1999) 490.
[29] M. Stobiecki, C. Malosse, L. Kerhoas, P. Wojlaszek, J. Einhorn, Phytochem. Anal. 10 (1999) 198.
[30] W. Andlaner, M.J. Martena, P. Furst, J. Chromatogr. A 849 (1999) 341.
[31] X.G. He, L.Z. Lin, L.Z. Lian, J. Chromatogr. A 755 (1996) 127.
[32] L.Z. Lin, X.G. He, M. Lindenmaier, J. Yang, M. Cleary, S.X. Qiu, G.A. Cordell, J. Agric. Food Chem. 48 (2) (2000) 354.
[33] X.G. He, L.Z. Lian, L.Z. Lin, M.W. Bernart, J. Chromatogr. A 791 (1997) 127.
[34] Y.Y. Lin, K.J. Ng, S. Yang, J. Chromatogr. A 629 (1993) 389.
[35] A. Kiehne, U.H. Engelhardt, Z. Lebensm. Unters. Forsch. 202 (1996) 48.
[36] M. Brolis, B. Gabetta, N. Fuzzati, R. Pace, F. Panzeri, F. Peterlongo, J. Chromatogr. A 825 (1998) 9.
[37] G. Piperopoulos, R. Lotz, A. Wixforth, T. Schmierer, K.P. Zeller, J. Chromatogr. B 695 (1997) 309.
[38] S. Gobbato, A. Griffini, E. Lolla, F. Peterlongo, Fitoterapia L17 (1996) 152.
[39] J.T. Dalluge, B.C. Nelson, J.B. Thomas, L.C. Sander, J. Chromatogr. A 793 (1998) 265.
[40] T. Goto, Y. Yoshida, M. Kiso, H. Nagashima, J. Chromatogr. A 749 (1996) 295.
[41] Y.Y. Lin, K.J. Ng, S. Yang, J. Chromatogr. 629 (1993) 389.
[42] R.G. Bailey, H.E. Nursten, I. McDowell, J. Sci. Food Agric. 66 (1994) 203.
[43] A. Kiehne, U.H. Engelhardt, Z. Lebensm. Unters. Forsch. 202 (1996) 299.
[44] A. Kiehue, C. Lakenbrink, U.H. Engelhardt, Z. Lebensm. Unters. Forsch. A 205 (1997) 153.
[45] K.D.R. Setchell, M.B. Welsh, C.K. Lim, J. Chromatogr. 386 (1987) 315.
[46] S. Barnes, M. Kirk, L. Coward, J. Agric. Food Chem. 42 (1994) 2466.
[47] R.M. Horowitz, S. Asen, Phytochemistry 28 (1989) 2531.
[48] J.F. Moran, R.V. Klucas, R.J. Grayer, J. Abian, J.B. Harborne, Phytochem. Anal. 9 (1998) 171.
[49] W.M. Keung, B.L. Valles, Proc. Natl. Acad. Sci. USA 90 (1993) 1247.
[50] W.M. Keung, B.L. Valles, Proc. Natl. Acad. Sci. USA 90 (1993) 10008.
[51] H. Rong, J.F. Stevens, M.L. Deinzer, L.D. Cooman, D.D. Kenkeleire, Planta Med. 64 (1998) 623.
[52] L.Z. Lin, X.G. He, M. Lindenmaier, G. Nolan, J. Yang, M. Cleary, S.X. Qiu, G.A. Cordell, J. Chromatogr. A (2000) in press.
[53] G.R. Waller, K. Yamasaki (Eds.), Saponins Used in Food and Agriculture, Advances in Experimental Medicine and Biology, Vol. 405, Plenum Press, New York, 1996.
[54] G.R. Waller, K. Yamasaki (Eds.), Saponins Used in Traditional and Modern Medicine, Advances in Experimental Medicine and Biology, Vol. 404, Plenum Press, New York, 1996.
[55] A. Griffini, E. Lolla, F. Peterlougo, Fitoterapia L18 (1997) 520.
[56] X. Wang, T. Sakuma, E.A. Adjaye, G.K. Shin, Anal. Chem. 71 (1999) 1579.
[57] R.B. Van Breemen, C.R. Huang, Z.Z. Ku, A. Rimando, H.H.S. Fong, J.F. Fitzloff, Anal. Chem. 67 (1995) 3985.
[58] M.P. Maillard, K. Hostettmann, J. Chromatogr. 647 (1993) 137.
[59] S. Fang, C. Hao, Z. Liu, F. Song, S. Liu, Planta Med. 65 (1999) 68.
[60] W.C. Chuang, D.S. Young, I.K. Liu, S.J. Shen, J. Chromatogr. A 755 (1996) 19.
[61] J.M. Chen, R.C. George, J.L. Weir, T. Leapheart, J. Nat. Prod. 53 (1990) 359.
[62] X.G. He, L.Z. Lin, L.Z. Lian, M. Lindenmaier, J. Chromatogr. A 818 (1998) 127.
[63] R. Hiserodt, T.G. Hartman, C.T. Ho, R.T. Rosen, J. Chromatogr. A 740 (1996) 51.
[64] P.A. Tarantilis, G. Tsoupras, M. Polission, J. Chromatogr. A 699 (1995) 107.
[65] N. Li, G. Lin, Y.W. Kwan, Z.D. Min, J. Chromatogr. A 849 (1999) 349.
[66] X.G. He, L.Z. Lin, M.W. Bernart, L.Z. Lian, J. Chromatogr. A 815 (1998) 205.

[67] X.G. He, M.W. Bernart, L.Z. Lian, L.Z. Lin, J. Chromatogr. A 796 (1998) 327.
[68] X.G. He, L.Z. Lin, L.Z. Lian, Planta Med. 63 (1997) 70.
[69] Y. Shao, K. He, B. Zheng, Q. Zheng, J. Chromatogr. A 757 (1997) 81.
[70] X.G. He, L.Z. Lian, L.Z. Lin, J. Chromatogr. A 757 (1997) 81.
[71] L.Z. Lin, X.G. He, L.Z. Lian, W. King, J. Elliott, J. Chromatogr. A 810 (1998) 71.
[72] A.P. Snyder (Ed.), Biochemical and Biotechnological Application of Electrospray Ionization Mass Spectrometry, ACS Symposium Series, No. 619, ACS, Washington, DC, 1995, p. 22.
[73] A.M. Gioacchinic, A. Roda, G.C. Galletti, P. Bocchini, A.C. Manetta, M. Baraldini, J. Chromatogr. A 730 (1996) 31.
[74] J.N. Alexander IV, C.D. Quinn, J. Chromatogr. A 647 (1993) 95.
[75] X.M. Wang, Y. Xue, T.H. Zhou, T. Sakuma, J. Food, Drug Anal. 5 (4) (1997) 337.
[76] S. Zhou, M. Hamburger, J. Chromatogr. A 755 (1996) 189.
[77] D. Temesi, B. Law, LC·GC 17 (1999) 626.
[78] J. Stockigt, J. Chromatogr. A 837 (1999) 83.
[79] O. Spring, H. Buschmann, B. Vogler, E.E. Schilling, M. Spraul, M. Hoffmann, Phytochemistry 39 (1995) 609.
[80] J.L. Wolfender, S. Rodriguez, K. Hostettmann, W. Hiller, Phytochem. Anal. 8 (1997) 97.
[81] Y. Zhao, A. Nookandeh, B. Schneider, X. Sun, B. Schmitt, J. Stockigt, J. Chromatogr. A 837 (1999) 83.
[82] J.R. Ioset, J.L. Wolfender, A. Marston, M.P. Gupta, K. Hostettmann, Phytochem. Anal. 10 (1999) 137.